Originally published in *Proceedings of the Fifth International Workshop on Compressible Turbulent Mixing*, ed. R. Young, J. Glimm & B. Boston.
ISBN 9810229100, World Scientific (1996).

Direct Numerical Simulation of Gravitational Turbulent Mixing*

A. A. Stadnik, V. P. Statsenko, Yu. V. Yanilkin,
and V. A. Zhmailo

Russian Federal Nuclear Center
Institute of Experimental Physics
Arzamas-16, Nizhegorodsky region,
Russia, 607200

This paper presents the results of direct (without empirical models) numerical simulation of turbulent mixing at the plane interface of two incompressible fluids (gases) with various densities moving with a constant acceleration.

The first similar studies were carried by Anuchina at al. [1] using the particle-in-cell method in 2D approximation. Then this approach was used by the authors of this paper to simulate the shear mixing [2]. The turbulence in these computations was treated as the result of random perturbations initially applied to the interface of two flows. The numerical simulation used 2D EGAK code [3]. The computational results were compared with the corresponding results obtained with the variant of semi- empirical turbulence theory with isotropic Reynolds tensor (model 1). In [4] similar computations were run to simulate the gravitational mixing.

This paper continues the studies in [4], using the direct numerical simulation with 2D and 3D methods [5],[6]. The data interpretation uses the version of semi-empirical theory (model 2) accounting for the anisotropy of Reynolds tensor.

1 Computation setup

The setup is similar to that of [4]: at initial time two half- spaces separated by the plane $z = z_c = 11$ are filled with perfect gases ($\gamma = 1.4$) at rest with the densities $\rho_1 = 3(z > z_c)$ and $\rho_2 = 1(z < z_c)$ the Atwood number is $A \equiv (\rho_1 - \rho_2)/(\rho_1 + \rho_2) = 0.5$. The gravity acceleration is directed from the heavy material to the light one, $g = 10$. At initial time random density perturbations $\delta\rho_1 = \pm\rho_1\delta$, where $\delta = 0.05$ ($\delta = 0.1$ in one of 2D computations) were applied to the interface (in a layer one cell thick). The computational domain is a cube with the side $\Lambda = 20$. The periodicity condition

*This work was supported by ISTC, Contract No 029.

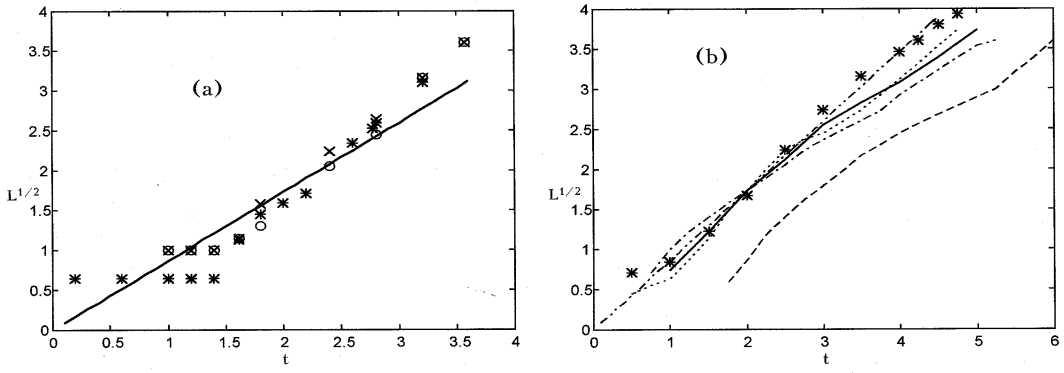

Figure 1: TMZ width as a function of time, *(a)* 3D calculation: $\circ$ fit to the semi-empirical profile ρ, $\times$ fit to the semi-empirical profile k, $*$ for the level $0.01psi$ ($\psi \approx abs[(\rho - \rho_{1,2})/(\rho_1 - \rho_2)]$); by experiment [9] *(b)* 2D calculations on the grid ($N_1 \times N_1$): $***$ $N_1 = 45$; $\cdots$ $N_1 = 100$, —— $N_1 = 100$, $- - -$ $N_1 = 200$, $- \cdot -$ $N_1 = 200$, $\delta = 0.1$; $- \cdot\cdot -$ by experiment [9].

with the period $\Lambda = 20$ was applied to outer domain boundaries parallel to the $\vec{g}$ while the rigid wall was taken for the others. The computational grid for 3D computations: $45 \times 45 \times 45$; the 2D grid ($N_1 \times N_1$) was varied from $N_1 = 45$ to $N_1 = 200$.

Note that the pressure value ($P \approx 10^3$) is such that for the turbulence the incompressibility condition was approximately met: $k = \xi Lg \ll \gamma P/\rho$, where $\xi = \text{const} \ll 1$, $L < \Lambda$, L — is the turbulent mixing zone (TMZ) width, k — is the turbulent energy.

2 Computational results

The flow evolution observed in 3D computations is generally similar to that of 2D computations [4]. The vortices grow with time and conversion to the self-similar mode is observed which for this problem is characterized by the linear variation law for $\sqrt{L(t)}$ (Figure 1). Here $L(t)$ was defined as the width of the self-similar profile (see below) closest to that obtained from the numerical calculation (Figure 2); profiles for $\rho(z) \equiv <\rho>$ and $k(z) \equiv < k >$ were taken from the numerical computations. Here and further the averaging ($<>$) was performed in the plane $z = \text{const}$ parallel to the interface plane.

The 3D structure of this flow is illustrated by the isolines of volume fraction $\beta = 0.5$ at time $t = 3.6$ located on various cross- sections $z = \text{const}$ (increases from the right to left and upward, $\Delta z = \text{const}$) in Figure 3. A similar pattern is shown for the cross-sections $x = 0.25$ and $y = 0.25$ (Figure 4).

As is seen from Figure 2 the relative profiles of k, ρ agree well with two versions

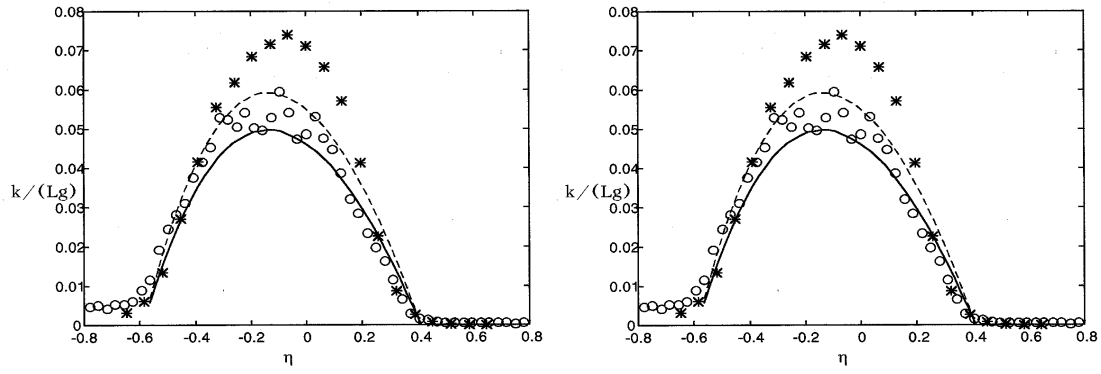

Figure 2: Turbulent energy profile (a) and density profile (b), $*$ 3D calculation, $t = 2.8$, $\eta = (z - z_c)/L$; $\circ$ 2D calculation, $t = 3.25$, $\eta = (y - y_c)/L$; semi-empirical models: —— [2] – – – this paper; coefficients: $\beta = 0.1$; $c_d = 0.25$; $c_2 - 0.56$; $c_3 = 0.65$; $k = 0.45$; $b = 1/6$; $a = 0.75$.

of semi-empirical theory; one of them [7] describing the isotropic turbulence within $k - D$ (a version of standard $k - \varepsilon$ model called model 1 below) and the other (see below) accounting for the anisotropy of Reynolds tensor using $k - D$ model (model 2) in the equilibrium approximation for k. Here the time $t = 2.8$ was chosen at the self-similar fragment of the mixing zone evolution. The self- similarity criterion can not be represented only by the linearity of $\sqrt{L(t)}$ because of low accuracy of its evolution. The additional criterion is where $E(t) = k_m/(Lg)$ because fixed in time; here $k_m \equiv \max(< k > (z))$. As is seen from Figure 5, showing this quantity as a function of $s \equiv (t/t_{\max})^2 (t_{\max} = \max(t))$ one can suggest that the self-similar mode also exists for $s \geq 0.25 (t \geq 1.8)$.

At the same time, the absolute mixing rate dL/dt differs in two models by about one order of magnitude which is shown by Figure 6 presenting the quantity $\Lambda_1 \equiv \frac{I}{t_{\max}} \sqrt{\frac{L_1}{Ag}}$ as a function of $(t/t_{\max})$. The derivative gives the quantity $\sqrt{\alpha_1}$ in expression for the coordinate of the mixing zone in heavy material: $L_1 = a_1 A g t^2$ [7]. The same figure shows the results of both of our computations and of similar 3D computations (two curves) [8]. In addition, the figure contains a straight line with the slope corresponding to the experimental data that are the most representative for the majority of known experiments. Globally our 3D calculations are close to this line though in the self-similar phase (see above) the slope is closer to the model 2. Youngs [8] believes that the self-similar mode is determined by the slope at later times which gives the value of the α_1 much lower that in experiments (note that it is close to model 1 data). However at this stage, the dimensions of the mixing zone are comparable with the distance to the computational domain boundary; at the same time at the initial stage the slope

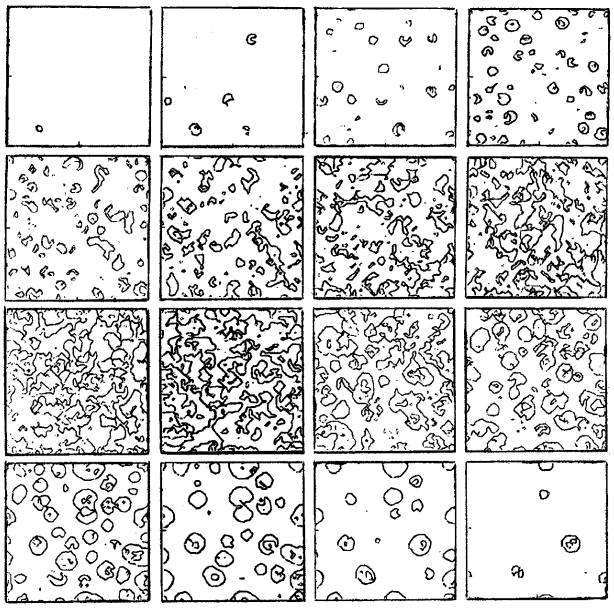

Figure 3: Isolines of volume fraction $\beta = 0.5$ in the planes $z = \text{const}$ at time $t = 3.6$, $\Delta z = \text{const}$.

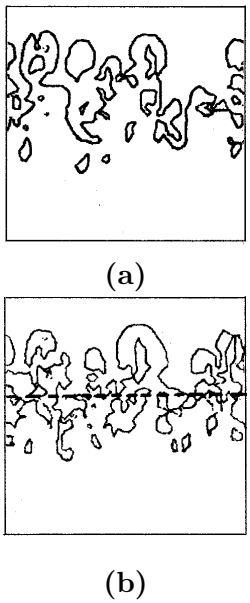

Figure 4: Isolines $\beta = 0.5$ in the planes: *a)* $x = 0.25$, *b)* $y = 0.25$.

of his curve is closer to data from [9] as shown by Figure 6. A motivated estimate of the self-similar stage position could be obtained if the function $E(t)$ is available. The same is true for the experimental data. For example, reference [10] reports the value of α_1 two times higher than in [9] (and this is close to results of model 2), however, because of non-constant g, the existence of the self- similar mode is still a question. In the experiment N422 from [11] where g is relatively constant α_1 is also close to [10]; however since the value of n is significantly higher (by orders of magnitude) as compared to our case, the question arises whether $\alpha_1(n)$ is constant.

The 3D computations clearly demonstrate the anisotropy of Reynolds tensor $R_{ik} \equiv < u'_i u'_k >$ and the longitudinal component of the turbulent energy (that is the diagonal portion of Reynolds tensor $E_{ii} = R_{ii/2}$ is much longer than each transversal component (Figure 7) and on average corresponds to the results of semi-empirical theory (model 2). However in this theory one has to take the coefficient $b = 1/6$ two times higher than in [12]. For shear flows, the difference is even greater (see below) that is b is non-universal parameter depending on Reynolds number. We also computed the quantity:

$$E_{jr}^{(i)} = \left\langle \left(u_j^{(i)}\right)^2 \right\rangle \Big|_r - \left\langle u_j^{(i)} \right\rangle^2 \Big|_r ; \qquad j = x, y, z; \qquad i = 1, 2, \ldots, N$$
$$E_{jr} = E_{jr}^{(i)} \Big|_r ; \qquad r = 2, 3, \ldots, N. \tag{1}$$

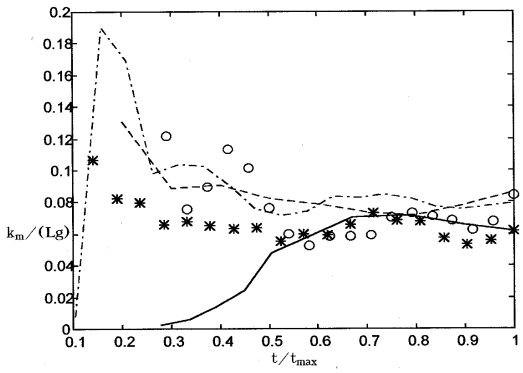

Figure 5: Maximum turbulent energy as a function of time, —— 3D calculation; 2D calculations: — · — $N_1 = 100$, – – – $N_1 = 100$, ∘ $N_1 = 200$, ∗ $N_1 = 200$, $\delta = 0.1$

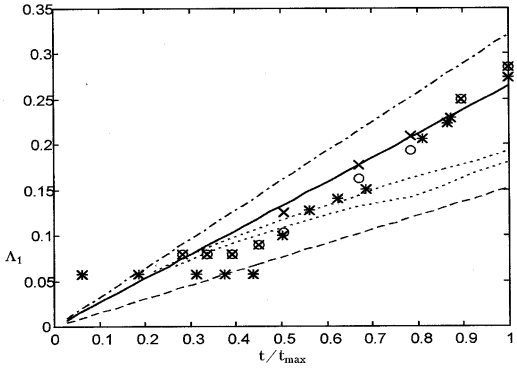

Figure 6: Coordinate of the light material in the heavy one, —— by experiment [9] 3D calculations: ∗, ∘,× this paper, ··· results [8] semi-empirical models: – – – [2] — · —this paper.

Here the averaging $\langle\rangle$ is accomplished in the i layer (z) in the square with the side r and further proceeds over all squares with the given r for the entire i layer; the results are shown in Figure 9 (where $K = 2\pi/l$, $l \equiv rh$, h — is the cell size) versus the Kolmogorov spectrum.

It is seen that in the mixing zone the spectrum of total energy $E_l = E_{lx} + E_{ly} + E_{lz}$ is very close to Kolmogorov value $\left(\lg E_{l(k)} = -2k/3 + \text{const}\right)$ for the small scale, however the anisotropy is retained till the least scales.

The 2D computations lead to a lower mixing rate as compared to three dimensions (Figure 1a, b). For the coarse grid ($N = 45$) the self-similar mode is achieved somewhat later when the mixing zone width L is comparable to the computational domain size. For a finer grid ($N = 100$, two runs with different realizations of initial disturbances), the origin of the self-similar mode corresponds to a relatively small width of the mixing zone, this is especially pronounced for the computations where the increase in amplitude of initial fluctuations ($\delta = 0.1$, $N = 200$) leads to faster turbulence evolution. This is confirmed by Figure 5 for the function $E(t) = k_m/(\lg)$; its constant value E_0 is achieved much earlier in this calculation. Note also that in 2D computations $E(t)$ is initially great ($> E_0$ — see Figure 5); accordingly, the slope of $L(t)$ in also great; later it decreases; in 3D case initially $E(t) < E_0$ and the slope of $L(t)$ increases.

The mixing rate obtained from 2D computations is close to the data of experiments from [13] (the straight line in Figure 8 with the slope $\sqrt{\alpha_1}$ determined by the value $\alpha_1 = 0.04$ obtained in [13]) with the setup similar to the 2D case. Note that in similar 2D computations [4] the mixing rate is significantly higher (at least with a factor of 2)

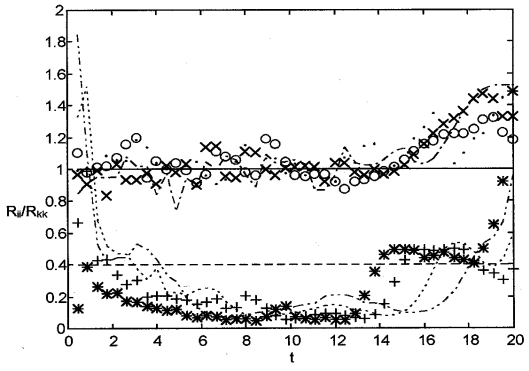

Figure 7: Reynolds-tensor anisotropy. 3D calculation: R_{xx}/R_{yy}, $\circ$ $t = 2.4$, $\times$ $t = 2.8$, –·– $t = 3.2$, $\cdots$ $t = 3.6$, R_{xx}/R_{zz}, $*$ $t = 2.4$, $+$ $t = 2.8$, $\cdots$ $t = 3.2$, –··– $t = 3.6$, semi-empirical model 2: —— R_{xx}/R_{yy}, – – – R_{xx}/R_{zz}.

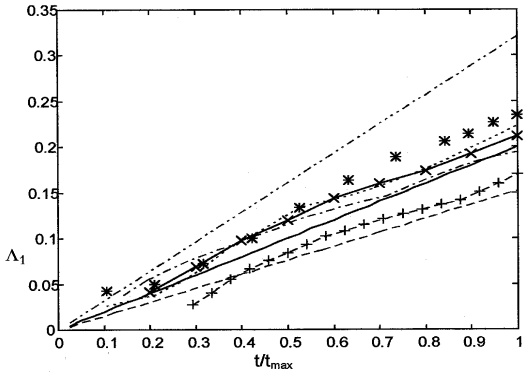

Figure 8: Light material coordinate in the heavy one, —— by experiment [13]; 2D calculations: $*$ $N_1 = 45$, $\cdots$ $N_1 = 100$, $x - x$ $N_1 = 100$, $+ - +$ $n_1 = 200$, —— · $N_1 = 200$, $\delta = 0.1$; semi-empirical models: - - - model 1, –··– model 2.

which can indicate that it is not sufficiently close to the self-similar mode.

As shown by Figure 2, the relative profiles of k, ρ in 2D computations (with $N_1 = 200$, $\delta = 0.1$) demonstrate much better agreement with the version of semi-empirical theory as compared to 3D case which can be explained by a finer grid.

Note that both 2D and 3D computations (in agreement with models 1 and 2) gives the ratio of coordinates of heavy material in the light one and light material in the heavy one $\Lambda_2/\Lambda_1 \approx 1.5$ which is greater then in [8],[9] (≈ 1.15).

For the same 2D case, Figure 9 shows the spectrum of turbulent energy (more precisely, diagonal components of Reynolds tensor) that is (1) where the averaging is accomplished over a segment rather than over the square like in 3D case. It is seen that for small scale the spectrum is close to the known spectrum $\left(\lg E_{l(k2)} = -2k + \text{const}\right)$ — 2D analog of Kolmogorov spectrum.

3 Semi-empirical theory (model 2)

The variant of theory of type [12],[14] accounting for Reynolds tensor anisotropy gives the equations:

$$\frac{\partial w}{\partial t} = -\frac{\partial R_1}{\partial z} \tag{2}$$

$$R_{12} \equiv \left\langle u'_y u'_z \right\rangle = R_1 = -DB_1 \frac{\partial \rho}{\partial z}; \tag{3}$$

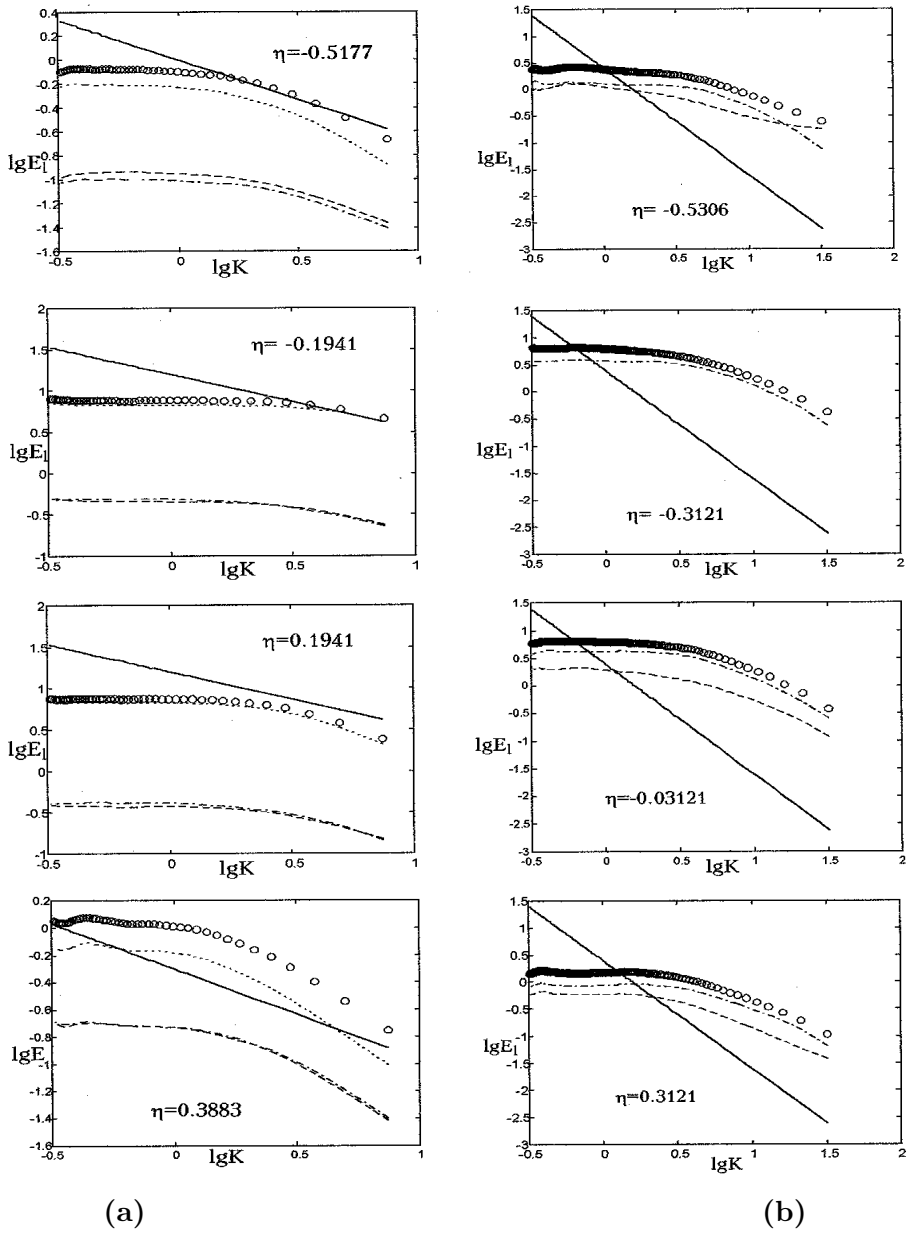

Figure 9: Turbulent energy spectrum, *a)* 3D calculation ($t = 2.8$), $\eta \equiv (z - z_c)/L$: $\circ$ E_l, - - - E_{lx}, $\cdots$ E_{ly}, ... E_{lz}; — $E_{l(K3)}$. *b)* 2D calculation ($t = 3.25$), $\eta \equiv (y - y_c)/L$: $\circ$ E_l, - - - E_{lx}, $-\cdot-$ E_{ly}, —— $E_{l(K2)}$.

$$B_1 = \frac{1/3 - b + 3b\varsigma}{a/2}; \quad \varsigma \equiv 1 + 1/k$$
$$k = \sqrt{\frac{g_{0z} R_1 D}{3b\rho}}; \quad g_{0z} \equiv g_z - \frac{d\nu_z}{dt} = \frac{1}{\rho}\frac{\partial p}{\partial z} \tag{4}$$

the equation for the turbulent diffusion coefficient D has the form:

$$\frac{dD}{dt} = \frac{D}{\epsilon}\frac{c_3 g_0 R_1}{\rho} + \frac{D}{\rho}\frac{\partial \rho}{\partial z}\frac{dD}{\partial z} + \frac{c_d}{\rho}\frac{\partial}{\partial z}\left(D\rho\frac{\partial \rho}{\partial z}\right) - 0.9c_2 b\epsilon \tag{5}$$

where : a, b, c_d, c_2, c_3 — are semi-empirical coefficients.

For the self-similar mode the solution is found by using the approximation:

$$Z \equiv (d\Psi/d\eta)/\Psi = \text{const}, \tag{6}$$

where the self-similar variable $\eta \approx (z/(gt^2))$; the solution has the same form as in [7] in our case:

$$\widetilde{k} = \frac{b(3c_3 - 0.9c_2)}{3 + 2c_d/B_1}. \tag{7}$$

4 Conclusions

The main results of this work are as follows:

The direct numerical simulation on 3D geometry was performed for the gravitational turbulent mixing that is hydrodynamic equations were solved without any phenomenology terms. For small scales Kolmogorov turbulence spectrum is reproduced. The TMZ growth rate does not disagree with the experimental data of various authors.

A similar study was performed in 2D geometry; a 2D analog of Kolmogorov spectrum is obtained for small scale. The TMZ growth rate is considerable lower than for 3D calculation and corresponds to the experiment [13] which is close to 2D case. It is shown that a good criterion for the solution transition to the self-similar mode, in addition to the linearity of $\sqrt{L(t)}$, is the constant value of $E(t) = k_m/(Lg)$; this is close in 3D and 2D computations.

A variant of semi-empirical model is formulated for the calculation of the flow under consideration with Reynolds tensor anisotropy and self-similar solution is obtained for this model.

The variant of semi-empirical method allows to give a more representative description of the corresponding experiments as compared to [6] with the isotropic Reynolds tensor; it agrees well with 3D computations.

The issues addressed in this paper need further clarification which may require similar studies on finer grids and with other numerical methods.

References

[1] N. N. Anuchina, Yu. A. Kucherenko, V. E. Neuvazhaev, V. N. Ogibina, L. I. Shibarshov, V. G. Yakovlev. Izv. AN SSSR, MZhG (in Russian), N6, pp.157-160, 1978.

[2] S. M. Bakhrakh, V. A. Zhmailo, V. P. Statsenko, Yu. V. Yanilkin. Numerical simulation of turbulent mixing in shear flows. Chisl.met.mekh. splosh. sredy, Novosibirsk, v.14 (in Russian), N2, pp.11-27, 1983.

[3] S. M. Bakhrakh, Yu. P. Glagoleva, M. S. Samigulin, V. D. Frolov, N. N. Yanenko, Yu. V. Yanilkin. Gas-dynamic flow computations with the method of concentrations. DAN SSSR (in Russian), v.257, N3, pp.566-569, 1981.

[4] V. A. Andronov, S. M. Bakhrakh, V. V. Nikiforov, Yu. V. Yanilkin. Numerical simulation of some turbulent flows in 2D turbulence approximation, Izv. AN SSSR, MZhG (in Russian), N6, pp.20-26, 1984.

[5] A. A. Shanin, Yu. V. Yanilkin. EGAK codes. Gas-dynamic difference schemes in Eulerian variables. VANT, Ser. Mat. mod. fiz. proc. (in Russian), N1, pp.24-30, 1993.

[6] A. L. Stadnik, A. A. Shanin, Yu. V. Yanilkin. Eulerian method TREK for 3D gas-dynamic flows in multicomponent medium. VANT, Ser. Mat. mod. fiz.proc. (in Russian), N4, 1994.

[7] V. A. Zherebtsov, V. A. Zhmailo, V. P. Statsenko. Self-similar solutions of semi-empirical equations for turbulent mixing in 1D time-dependent flows. Chisl. met. mekh. splosh. sredy, Novosibirsk (in Russian), t.15, N1, 1983.

[8] D. L. Youngs. Three-dimensional numerical simulation of turbulent mixing by Rayleigh-Taylor instability. Phys. Fluid A, 3, p.1312, 1991.

[9] Yu.A. Kucherenko, L. I. Shibarshov, V. I. Chitaikin, S. I. Balabin, A. P. Pylaev. Experimental study of the gravitational turbulent mixing self-similar mode. 3^{rd} International Workshop on The Physics of compressible turbulent mixing, Abbey of Royaumont (France), pp.345-356, 1991.

[10] A. M. Vasilenko, V. I. Olhovskaya, O. V. Burykov, V. G. Yakovlev. Experimental investigation for turbulent mixing of gases at the plane interface under the influence of the decelerating shock wave. 3rd International Workshop on The Physics of compressible turbulent mixing, Abbey of Royaumont (France), pp.535-552, 1991.

[11] E. E. Meshkov and N. V. Nevmerzhitsky. About turbulent mixing dynamics at unstable boundary of liquid layer, accelerated by compressed gas. 3rd International Workshop on The Physics of compressible turbulent mixing, Abbey of Royaumont (France), pp.467-475, 1991.

[12] W. S. Lewellen, M. E. Teske, C. P. Donaldson. Variable density flows computed by a second-order closure description of turbulence. AIAA Journal, v.14, N3, pp.382-387, 1976.

[13] M. J. Andrews and D. B. Spalding. A simple experiment to investigate two-dimensional mixing by Rayleigh-Taylor instability. Phys. Fluid A, v.2, pp.922-927, 1990.

[14] S. M. Bakhrakh, N. S. Darova, G. V. Zharova, V. A. Zhmailo, V. P. Statsenko. Turbulent and molecular mixing in thin vortex rings. VANT, Ser.: Teor. i Prikl. Fiz., N2, 1987.